UNIVERSITY OF PARDUBICE
FACULTY OF CHEMICAL TECHNOLOGY
Department of Physical Chemistry

Jana Romanová

Study of behavior of amorphous drugs

Theses of the Doctoral Dissertation

Pardubice 2022

Study program: **Physical Chemistry**
Study field: **Physical Chemistry**

Author: **Ing. Jana Romanová**
Supervisor: **prof. Ing. Jiří Málek, DrSc.**
Year of defence: 2022

Acknowledgement

I would like to thank my supervisor prof. Jiří Málek, DrSc and my specialists doc. Alena Komersová, PhD and Roman Svoboda, PhD for their assistance, support, valuable advice related to my research within the PhD study. This work has been supported by the pharmaceutical company Zentiva, k.s., which supplied APIs, other chemicals and provided instruments. Most of the measurements used in this work were done during my long-term fellowship in Zentiva k.s. I would like to thank to my consultants from Zentiva k.s., namely Tomáš Pekárek, Ph.D, Iva Obadalová and Lukáš Krejčík. I would like to thank Michal Šimek, PhD, and Ondřej Dammer, PhD, for knowledge support and measurement of X-ray powder diffraction methods and Jaroslav Havlíček, CSc., for knowledge support and measurement of NMR. I appreciate being a member of the Center for applied pharmaceutical research, i.e. The Parc. I would like to thank my colleagues from the research group of professor Málek, the research group of Alena Komersová and the department of preformulation and biopharmacy of Zentiva k.s. for their assistance and valuable advice. I would like to thank Dita Spálovská for language corrections and advice related to the processing of my dissertation.

This work has been supported by the Czech Science Foundation under project No. 17-11753S and by the projects LM2015082, CZ.02.1.01/0.0/0.0/16_013/0001829, and mainly by the Zentiva, k.s. I would like to thank the Center of materials and nanotechnology (under the project LM2018103) for measurement of SEM. The author would like to express her gratitude for research stay at National Institute for Materials Science (NIMS) in Tsukuba, Japan within the NIMS International Cooperative Graduate Program.

References

ROMANOVÁ, Jana. *Study of behavior of amorphous drugs.* Pardubice, 2021. 198 pages. Dissertation thesis (PhD.). University of Pardubice, Faculty of Chemical Technology, Department of Physical Chemistry, Supervisor Prof. Ing. Jiří Málek, DrSc.

Abstract

Nowadays, the low water solubility of active pharmaceutical ingredients (APIs) is one of the biggest pharmaceutical industry challenges. Almost 40 % of the marketed APIs and 90 % of the APIs being developed are nearly insoluble in water. A multifold increase in solubility might be achieved by the conversion of crystalline API to amorphous form. The increase may be up to 1000 times higher than the thermodynamic solubility of the API. Presented dissertation deal with the behavior of amorphous enzalutamide, and the chapter of results is divided into two parts. The first subchapter is about the preparation of the amorphous form and solid-state stability. The subject matter of this subchapter is a kinetic description using the macroscopic technique, i.e. differential scanning calorimetry. The crystallization behavior has been correlated with the results of short-term and long-term stability testing. The experiments confirmed the reliability of the theoretical prediction of crystallization. Equally important to solid-state stability is the behavior of the amorphous enzalutamide during its dissolution. Therefore, the second chapter of this work is devoted to the dissolution behavior of the amorphous enzalutamide and its ability to maintain oversaturated state. Amorphous enzalutamide was found to crystallize very rapidly, both in solid-state and during dissolution. This dissertation identified the most critical factors influencing the crystallization behavior of amorphous enzalutamide. Also, there was suggested a way to avoid or slow down crystallization of amorphous enzalutamide.

Abstrakt

Nízká rozpustnost farmakologicky účinných látek (API) je jedním z největších problémů, kterým v současnosti čelí farmaceutický průmysl. Téměř 40 % API uvedených na trh a 90 % API nacházejících se ve výzkumu je téměř nerozpustných ve vodě. Mnohonásobného zvýšení rozpustnosti je možno dosáhnout převedením krystalické API na amorfní formu. Toto zvýšení může až 1000krát převyšovat termodynamickou rozpustnost zkoumané API. Předložená disertační práce se zabývá chováním amorfního enzalutamidu, přičemž výsledky jsou rozděleny do dvou kapitol. V první kapitole je řešena příprava amorfního enzalutamidu a jeho pevnofázová stabilita. Předmětem této kapitoly je kinetický popis krystalizace pomocí makroskopických technik, v tomto případě pomocí diferenční skenovací kalorimetrie. Krystalizační chování připraveného amorfního materiálu bylo korelováno s výsledky krátkodobých a dlouhodobých stabilitních testů. Kinetické výpočty umožnily poměrně spolehlivě predikovat krystalizaci amorfního enzalutamidu. Neméně důležité je chování amorfního enzalutamidu během jeho rozpouštění, proto druhá kapitola této práce je věnována disolučnímu chování amorfního enzalutamidu a možnostmi udržení jeho přesyceného stavu. Amorfní enzalutamid byl shledán jako velmi rychle krystalizující API a to jak v pevné fázi, tak během disoluce. V této disertační práce

byly identifikovány vlivy, které nejvíce ovlivňují krystalizační chování amorfního enzalutamidu, a možnosti jakými se jeho krystalizaci vyhnout či ji zpomalit.

Keywords
amorphous enzalutamide, glass-forming ability, the physical stability of amorphous API, prediction of the crystallization, dissolution behavior of enzalutamide

Klíčová slova
amorfní enzalutamid, sklotvornost, fyzikální stabilita amorfní API, predikce krystalizace, disoluční chování enzalutamidu, extruze z taveniny

Table of Contents

Introduction and goals of dissertation

The poor solubility of APIs is the limiting factor of their usage. This issue is related to 90 % of drugs in the development and 40 % of drugs currently in the global market. The solubility of APIs may increase by particle size reduction or by the formation of salts of the API (***A**ctive **P**harmaceutical **I**ngredient*). However, the solubility increase is mostly not significant. In the previous decades, considerable research and development were devoted to amorphous APIs.

Amorphous matter does not contain a long-distance arrangement. Therefore, the apparent solubility increases due to the absence of energy needed to break the crystalline lattice. The dissolution of the amorphous form leads to supersaturation. The supersaturation is a metastable state when the crystallization or phase separation occurs quickly. The phase separation is the state represented by API´s coagulates of hundreds of nanometers in size. These coagulates most probably serve as reservoirs of API available for absorption to systematic circulation. Still, there is an option for holding the supersaturation state, e.g. by surfactants or polymers, which should be included in the formulation.

Nevertheless, the amorphous form has higher Gibbs energy in comparison with the crystalline state; therefore, the amorphous form is significantly unstable. The risk of crystallization may occur during the preparation of amorphous API, its storage or dissolution. Understanding influences affecting the crystallization of API is necessary to achieve a stable amorphous dosage form.

The author´s doctoral study was focused on several projects dealing with amorphous APIs. Due to the large-scale experimental results, the presented dissertation theses deal only with two selected topics. The first one is the crystallization in the solid state. The studied API was the enzalutamide. The crystallization kinetics was studied by differential scanning calorimetry. The reliability of the predictions based on the non-isothermal data was investigated. The non-isothermal experiments are quite fast and that is their advantage because they can save time and costs related to the development of stable amorphous forms. The crystallization of the enzalutamide was studied regarding the influence of temperature, humidity and mechanical stress. The presented dissertation showed the accuracy of these predictions. The second topic was an investigation of the dissolution behaviour of amorphous and crystalline enzalutamide. The aim of this study was to determine the true benefit of using the amorphous form of enzalutamide instead of the crystalline form. Studying and understanding the dissolution kinetics was an important part of this topic.

The dissertation structure has a classical formal arrangement: Theoretical part, Experimental part, Results and Discussion, Conclusion. The theoretical part was elaborated as a comprehensive overview of wide-area related to topics of dissertation – The general theoretical part deals with the amorphous APIs and their bioavailability, preparation, and stability. In addition, the theory describes the kinetic calculations and

the basis of the experimental methods used in the dissertation. The experimental part and chapter Results and Discussions are divided into two subchapters corresponding to the studied topics, i.e. solid-state stability of amorphous enzalutamide and dissolution behavior of enzalutamide. Each of these subchapters is concluded separate conclusion summarizing each chapter as a part of the chapter Results and Discussion. The Conclusion chapter is again divided into two subchapters. The subchapter is drawn from the Results and Discussion chapter, and the second subchapter summarizes the main conclusions of the other topics addressed within the PhD study.

Theses of the dissertation contains a short theory related to amorphous drugs, main goals of dissertation, experimental part and main results and conclusions of dissertation.

1. Theoretical part – a brief overview

This chapter is a short extract of the theoretical part of the dissertation.

1.1. Amorphous APIs

The amorphous form of API lacks a crystalline lattice and exhibits only a short-distance arrangement. The apparent solubility of amorphous API is higher than the solubility of its crystalline counter partner due to the absence of the energy needed to break the crystalline lattice. The transformation of crystalline API to an amorphous form is advantageous for poorly soluble APIs, i.e. API classified as II. or IV. Class according to BSC (biopharmaceutics classification system). [1–4].

Amorphous APIs could be prepared using various methods, which may be divided into two groups of preparation: thermodynamic and kinetic. Thermodynamic preparation uses disorderly structure as the source material, i.e. melt, solution of API. The principle of the method is fast cooling of the melt or rapid removal of the solvent. These methods include hot melt extrusion, spray drying and freeze-drying. In the case of kinetic way of preparation, the starting material is ordered structure, i.e. crystalline form. The principle is the mechanical activation of defects in the crystalline grid where the entropy increases until the amorphous state is reached. Grinding and milling are part of the kinetic methods of preparation[1–4].

If the conversion of crystalline API to the amorphous form is considered, then the following characteristics should be investigated:

1. The ability of the API to form amorphous phase – i.e. glass-forming ability (abbr. GFA)
2. The physical stability of the prepared amorphous API – i.e. crystallization kinetics
3. The stability of amorphous form in supersaturation state during the dissolution – precipitation (crystallization or coagulation of amorphous form)

All three areas are very important. The simple experiment in DSC (differential scanning calorimeter) can verify the first point (glass-forming ability): heating through the melting point/cooling of the melt/second heating of prepared form. Baird et al.[5] proposed this methodology, and they divided the APIs into three general classes based on the characteristics that the most influence GFA. The molecular weight of API, the number of rotation bonds, and the difference in Gibbs energy between the amorphous and crystalline phases have the greatest influence on GFA. The three classes of APIs classified according to GFA are as follows:

I. Class of API according to GFA

These APIs crystallize during the cooling of the melt. This group is divided into two subgroups: I.A and I.B. APIs of I.A class crystallizes even during fast cooling (cooling by the liquid nitrogen). APIs of I.B class crystallizes only when the cooling rate is low, i.e. 20 $°C \cdot min^{-1}$. The amorphous API can be prepared only from the representants of class I.B. However, amorphous APIs prepared from APIs class I are

unstable. Generally, APIs of class I. are small simple molecules with low molecular weight and a low number of rotation bonds. The examples of class I are ibuprofen, caffeine, griseofulvin, and so on[5,6].

II. Class of API according to GFA

These APIs can be prepared even using a low cooling rate, i.e. 1 °C·min^{-1}. The significant DSC characteristic is exothermic crystallization during the amorphous form's reheating (second heating of the cycle). The representatives of the group are acetaminophen, celecoxib, D-salicin, and so on[5,6].

III. Class of API according to GFA

These APIs do not crystallize during the slow cooling and even during the subsequent reheating of the amorphous form (speaking of DSC method – heating/cooling/heating cycle). The significant characteristic of APIs of class III is the highest molecular weight and number of rotation bonds compared to classes I. and II. The molecular weight of APIs of class III generally is higher than 300 g·mol^{-1}. These APIs should form the most stable amorphous form compared to other classes (according to GFA), but this is still not the rule of thumb for all representatives. The representatives of class III. are indomethacin, ketoconazole, intraconazole, ketoprofen and so on[5–7].

The classification mentioned above is based on differential scanning calorimetry. The behavior of amorphous APIs can be different regarding the preparation method (spray drying, freeze-drying, milling etc.)[7]. For more about glass–forming ability and its relation to attributes of APIs, see the full version of the dissertation. The second important area regarding amorphous APIs is their physical stability. The stability of APIs in amorphous form is connected to GFA, as was mentioned above. The amorphous state physical stability (glass stability, abbr. GS) is related to crystallization tendency. The API is stable in the amorphous form if the crystallization tendency is low. Modelling of crystallization is a very important discipline that could lead to precise prediction of crystallization, i.e. prediction of the stability of amorphous form. Findings related to the generalization of the behavior of amorphous forms is crucial for the pharmaceutical industry.

The modelling of crystallization behavior is usual in the case of inorganic compounds (inorganic glasses). However, the crystallization behavior of organic compounds (e.g. APIs) is different from inorganic compounds due to weak intermolecular instead of covalent bonds. The stability criteria used in the case of inorganic compounds (reduced glass transition temperature T_{rg}, criterion Hruby K_H, criterion Lu and Liu K_{LL}, criterion Saad and Poulian K_{SP}, fragility etc.) are not enough precise in the case of organic compounds (e.g. APIs). Only the correlation of GFA, GS with the organic compound (API) properties have been determined. The GFA, GS of API depend on the molecular weight of API, the number of rotation bonds and the value of the difference of Gibbs energy between the amorphous and crystalline state ($\Delta G_{a\rightarrow c}$). Based on these properties, the classification system mentioned above was established. Generally, the most stable amorphous APIs had molecular weights higher than 300 g·mol^{-1} and crystallization temperature higher than 120 °C [cit. 5–10]. Until this

time (to the authors' knowledge), any exact method for predicting crystallization does not exist, even though many scientists are involved in this discipline. The isothermal experiments at storage temperatures are time-consuming. Therefore, this work is devoted to study the crystallization of amorphous enzalutamide by non-isothermal experiments in differential scanning calorimeter, which may speed up the development of stable amorphous forms. The kinetic calculations applied to non-isothermal data are shown in chapter 1.2.

The third area of interest in the field of amorphous APIs is their dissolution behavior. Amorphous APIs shows higher apparent solubility than crystalline APIs owing to high Gibbs energy ($\Delta G_{a\rightarrow c}$), high entropy ($S$), higher wettability etc. The concentration in dissolution media usually increases after 10–15 minutes of dissolution experiment. This concentration is usually several times higher than the solubility of the crystalline form. The immediate increase of concentration is called the "spring effect ". Two events can happen after the „spring effect". Firstly, the concentration may decrease to the concentration of crystalline form due to crystallization. The second option is the maintenance of the higher concentration, which is called the "parachute effect ". The "parachute effect "is the consequence of the rising of the metastable polymorph (having higher solubility than original crystalline form) or stabilization of the supersaturation state by additives (polymers, clusters etc.)[2,11]. The desired effect is the maintenance of the supersaturation state. This dissertation investigates the dissolution behavior of amorphous enzalutamide itself and amorphous enzalutamide in the presence of the polymer. The aim of the study mentioned above was the mathematical description of dissolution kinetics and proof of the difference between the amorphous and crystalline forms of enzalutamide.

1.2. Crystallization kinetics

The amorphous form of API is unstable and tends to crystallize. Therefore, the prediction of crystallization of amorphous APIs is one of the essential disciplines. However, the prediction is a very complex field, and the result is influenced by the storage conditions of API (temperature, humidity, mechanical stress), preparation method (solvent evaporation, quench–cooling, etc.), and properties of the drug itself (molecular weight, number of rotatable bonds, temperature of glass transition, crystallization temperature). The crystallization data in this study were observed by differential scanning calorimetry. The differential scanning calorimetry is based on the measurement of the heat evolved during the crystallization process. The methodology below is used mainly in the field of inorganic glasses, and it will be applied to the crystallization kinetics of API of II. class according to GFA. The crystallization can be described by the determination of parameters of standard DSC equation (1)[12]:

$$\varphi = \frac{dQ}{dt} = \Delta H \cdot A_f \cdot e^{-\frac{E}{R \cdot T}} \cdot f(\alpha) \quad (1)$$

where φ means heat flow in the units of $J \cdot s^{-1}$ g^{-1}, ΔH is the enthalpy of a monitored process in the units of $J \cdot g^{-1}$, A_f is the frequency factor in s^{-1}, E means the activation energy of monitored process in $J \cdot mol^{-1}$, R is the universal gas constant, i.e. 8,314 $J \cdot mol^{-1} \cdot K^{-1}$, T is the temperature in the units of Kelvin, f(α) is the kinetic model appropriate for the monitored process.

By quantifying the parameters of this equation, it is possible to describe the crystallization kinetics of amorphous APIs and use them to predict isothermal crystallization. As it is clear from the DSC equation, the enthalpy of the process, activation energy and parameters of the chosen kinetic model should be determined. The enthalpy of the process are obtained by integration of the crystallization peak area, and the values are influenced by the type of baseline (linear, B-spline, area–proportional, etc.)[12]. The activation energy can be determined by the various methods shown in the section below.

1.2.1. Determination of activation energy

The various methods determining the activation energy depend on the experimental conditions used for gaining of crystallization data (isothermal, non-isothermal measurement). The disadvantage of the isothermal experiment is the temperature range when the capturing of the whole process is time-consuming in the case of the lower temperatures. However, in case of higher temperatures, the process can be finished before achieving the isothermal conditions. In this dissertation, non-isothermal methods were used. The following methods are marked as "model-free methods", because the kinetic model is not necessary for determination of the activation energy. The DSC data should be acquired by the set of different heating rates $\boldsymbol{q}^+$. The usual principle of these methods is the shift of the temperature the crystallization peak maximum (or temperature corresponding to a certain level of conversion) with the increasing value of the heating rate. The following methods are divided into two groups. The first one declares that the crystallization mechanism does not change during the crystallization process, and the degree of conversion achieved in the maximum of the crystallization peak is the same for all heating rates. The second

one determines the activation energy for certain conversions, and the result is the dependency of activation energy on conversion[12].

1) Group of methods – These methods assume the same degree of the conversion achieved in the maximum of the crystallization peak for all heating rates (experimental conditions during DSC measurement). In other words, the crystallization mechanism does not change in the particular temperature or time range (depending on the DSC regime – isothermal, non-isothermal). Experimental data are observed by application of different linear heating rates $\boldsymbol{q}^+$ during the DSC experiment. One representatives of the presented methods is the Kissinger method (2)[13,14]:

$$ln\frac{q^+}{T_p^2} = -\frac{E}{R \cdot T_p} + K \quad (2)$$

where q^+ means the heating rate in °C·min^{-1}, E is the activation energy in J·mol^{-1}, T_p is the temperature of the maximum of the crystallization peak, R is the universal gas constant in J·mol^{-1}·K^{-1}, and K is the constant.

The activation energy is gained from the Kissinger method[13] (2) by plotting the right part of the equation $ln\frac{q^+}{T_p^2}$ in dependency on $\frac{1}{T_p}$ or $\frac{1000}{T_p}$.

2) Group of methods – These methods determine activation energy for a certain degree of conversion. Data are obtained in the same manner as in the previous case, i.e. by different linear heating rates $\boldsymbol{q}^+$. Note, conversion presents the portion of recrystallized amorphous material. In this case, the particular conversion is achieved during the non-isothermal DSC experiment. The total area of the crystallization peak means 100 % of conversion ($\boldsymbol{\alpha}$). In this method, the temperature $\boldsymbol{T_\alpha}$ at which particular conversion is achieved should be determined. $\boldsymbol{T_\alpha}$ have to be determined for each heating rate[15]. The representant of the methods of this group is Kissinger–Akahira–Sunose method[15] (3):

$$\ln\left(\frac{q^+}{T_\alpha^{1,92}}\right) = -1{,}0008 \cdot \frac{E\alpha}{R \cdot T_\alpha} + K'' \quad (3)$$

where $\boldsymbol{q}^+$ means the heating rate in °C·min^{-1}, $\boldsymbol{E}$ is the activation energy in J·mol^{-1}, $\boldsymbol{T_\alpha}$ is the temperature at which particular conversion is achieved, $\boldsymbol{R}$ is the universal gas constant in J·mol^{-1}·K^{-1}, and $\boldsymbol{K}$ is the constant.

1.2.2. Determination of the kinetic model

The other step of kinetic analysis is the choice of the kinetic model and determination of its parameters. The so-called master plot, i.e. z(α), y(α) = f[α] is used for the selection of the appropriate kinetic model. The shape of the master plot - z(α), y(α) = f[α] and values of the maximum of these characteristic functions are significant for the particular model. More information about the master plot is available in the full version of the dissertation. The kinetic models used in this dissertation are following:

Šesták–Berggren model

This model is an autocatalytic and universal model with two parameters; see equation (4). Parameters of the model do not have physical meaning. Still, the model is the most used kinetic model[16,17].

$$f(\alpha) = \alpha^M \cdot (1-\alpha)^N \quad (4)$$

where ***f(α)*** represents kinetic model, ***M*** and ***N*** are parameters of Šesták-Berggren model and ***α*** is the conversion.

JMA

The JMA model is the special case of the Šesták–Berggren model. This model is one of the most used models for the description of crystallization in glass-forming materials. Equation (5) represents the JMA model[17,18]:

$$f(\alpha) = m \cdot (1-\alpha) \cdot [-\ln(1-\alpha)]^{1-\frac{1}{m}} \quad (5)$$

where ***f(α)*** represents kinetic model, ***m*** is the parameter of JMA model and ***α*** is the conversion.

n–order reaction model

This model is an autocatalytic model, and its mathematical formulation is shown as equation (6)[17]:

$$f(\alpha) = (1-\alpha)^n \cdot (1+K\alpha) \quad (6)$$

where ***f(α)*** represents kinetic model, ***n*** and ***K*** are parameters and ***α*** is the conversion.

1.3. Dissolution kinetics

Dissolution testing has been for a long time one of the most used methods in the pharmaceutical development and quality control department of pharmaceutical companies. Besides, dissolution testing is crucial for regulation authorities who approves drug release on the market. The authorities as FDA, EMA dictates the way of proper implementation of the dissolution testing[19–21]. The dissolution profile brings many important information like the type of the API release from a dosage form (i.e. immediate, controlled), the type of the controlled release of the API (i.e. sustained, delayed, pulsatile), the release mechanism of the API from the dosage form (swelling, diffusion, erosion etc.). The visual changes of the drug dosage form during the dissolution are also useful for clarifying the events occurring on the dissolution profile. Some of these are disintegration, swelling or floating of the tablet. Dissolution behavior markedly influences the bioavailability of the API.

Dissolution testing is carried out in glassy bottles equipped with a paddle/basket. The defined volume of the dissolution media is sampled in the predetermined time intervals. The amount of the dissolved API is determined over the time, dissolution curve. In this dissertation, closed system is used when the sampled dissolution media is not replaced by the fresh dissolution media. The dissolution methods used in this dissertation was the paddle method (USP II) and apparent intrinsic dissolution method paddle with the API disc (USP VI)[22]. More information about experimental methods

used in this dissertation is in the chapter Methodology and in the full dissertation version.

The dissolution curve/profile is the dependence of the released/dissolved API on time. For the dissolution analysis, the mathematical models are applied to the dissolution curve. There is a variety of mathematical models for the description of the dissolution profile. The models used in this study are following:

Zero-order kinetics

The release/dissolution of the API is independent of the initial dose of the API in the dosage form, and the API is constantly releasing/dissolving on a time-dependent basis. The zero-order kinetics is the ideal case of the behavior of the dosage forms with the controlled release because then the stable plasmatic concentration is achieved. The zero–kinetics follows equation below[23,24]:

$$A_t = k_0 t \quad (7)$$

where A_t is the amount of API released in time t, k_0 is the rate constant in units of amount of the API·time^{-1}.

First–Order kinetics reaction

The dissolution rate is dependent on the amount of the API in the drug dosage form, and the dissolution rate decreases with time. The highest amount of the released API (*in vivo*) is achieved immediately after administration of the drug, and then the amount of released API decreases. This type of release/dissolution is not convenient for controlled release. The equation (8) representing first–order kinetics is shown below[24,25]:

$$A_t = A_\infty\left(1 - exp(-k_1 t)\right) \quad (8)$$

where A_r represents the amount of the API released/dissolved in time t, A_∞ represents the maximum of the releasable/dissolvable amount of the API, k_1 is the rate constant in the units of time^{-1}.

Weibull model

The Weibull model is a statistical model whose parameters k_w, β do not have physical meaning. This model can be represented by the equation (9) as follows[24,26]:

$$A_t = A_\infty\left(1 - exp\left(-k_w(t - T_t)^\beta\right)\right) \quad (9)$$

where A_r represents the amount of the API released/dissolved in time t, A_∞ represents the maximum of the releasable/dissolvable amount of the API, k_{KP} is the rate constant in the units of time^{-n}, n is the release exponent.

Korsmeyer–Peppas model

This model enables the determination of the release mechanism of the releasing of the API from the polymer carriers. The model is valid for the first 60 % of the released/dissolved API. The Korsmeyer–Peppas model follows equation (10)[27]:

$$\frac{M_t}{M_\infty} = k_{KP} t^n \quad (10)$$

where M_r represents the amount of the API released/dissolved in time t, M_∞ represents the maximum of the releasable/dissolvable amount of the API, k_w is the rate constant in the units of time$^{-\beta}$, T_t is the delay in the API release at the start, β parameter characterizes the shape of the exponential curve.

2. Marketed amorphous drugs

Despite the amorphous APIs' low stability compared to crystalline APIs, amorphous APIs are included in several drug products. In 2007, about 16 drug products contained APIs in the form of solid dispersion, and five drug products contained pure amorphous API. In the case of solid dispersions, nine APIs belong to class III according to GFA, and two APIs belong to class II and one API to class I according to GFA. Obviously, even the poor glass former, i.e. API of class I can be used in the drug dosage form if the appropriate excipients are chosen[28].

The APIs used in pure amorphous form are cefuroxin axetil, nelfinavir mesylate, chinapril hydrochloride, rosuvastatin calcium and zafirlukast. Only for two of them, the class GFA was determined, i.e. class III. Other APIs decompose during the melting, and the class according to GFA was not possible to be determined. It is clear that the usage of the appropriate excipients, method of the amorphization, type of the dosage form, appropriate packaging and storing conditions can lead to a stable amorphous dosage form[28].

3. Methodology

This chapter shows the preparation of the amorphous material by hot-melt extrusion and experimental method only for two main characterization techniques, i.e. differential scanning calorimetry and dissolution testing. The amorphous enzalutamide was prepared by hot melt extrusion and by spray drying and vapor evaporation. The detailed crystallization behavior of the mentioned materials is described in the full version of the dissertation.

3.1. Hot melt extrusion

The amorphous form was prepared by hot melt extruder Three-Tec (GmbH, Switzerland) with two co-rotating screws. The input material for hot melt extrusion was crystalline enzalutamide polymorphic form R1 with particles smaller than 500 μm. The material was extruded at 230 °C with a rotation speed of 100 min^{-1}. The feeding rate was 20 g·hod^{-1}. Two bathes of the material were prepared: one was cooled

to room temperature, and the second one was cooled down to the liquid nitrogen temperature.

3.2. Differential scanning calorimetry – Study of the crystallization behavior

The crystallization behavior of amorphous API was studied using differential scanning calorimeter DSC Q2000 (TA Instruments, USA) equipped with a cooling accessory. The device was calibrated using standards of indium and zinc. The measurement was carried out under the flow of nitrogen (purity 99.999 %) about 30 $mL \cdot min^{-1}$. Samples (1 – 2 mg) were hermetically sealed in the DSC low-mass T-Zero aluminum pans. The samples were heated by different heating rates (0.5; 1; 2; 5; 10 and 20 $°C \cdot min^{-1}$).

3.3. Dissolution testing

The aim of the dissolution testing was to determine the advantage of the usage of the amorphous form of the enzalutamide instead of crystalline enzalutamide. The apparent intrinsic dissolution verified the difference between the intrinsic dissolution rate of amorphous and crystalline enzalutamide. The intrinsic dissolution rate is independent of the value of the specific surface area which is exposed to dissolution. After that, the dissolution in powder form was done to identify the influence of the specific surface. The results showed the need for the addition of the polymers, so the granules with the polymer were prepared. The desired release kinetics in the final formulation is immediate release.

3.3.1. Apparent intrinsic dissolution

The dissolution testing was carried out using a dissolution device/automatic titrator Sirius in Form 1501013 (Sirius Analytical Instruments Ltd., Great Britain). The samples were formed into a disc (diameter about 8 mm) using compression force 110 N (exposition time - 2 minutes). The aim was to prepare a smooth surface without any discrepancies. The dissolution method was the paddle method with the disc (USP VI) The samples were inserted into the 40 mL of the dissolution medium, which was phosphate buffer 72,2 mM about pH 6.8 containing 0,2 w/V % of SLS (sodium lauryl sulphate). The temperature of the dissolution medium was 37 ± 0.5 °C. The rotation speed was 100 min^{-1}. The experiment lasted about 40 minutes. The content of API was analyzed online UV-VIS detection every 30 seconds at 270 nm.

3.3.2. Dissolution of amorphous API in powder form

The dissolution testing was carried out using a dissolution device DS-11 SOTAX (SOTAX Pharmaceutical Testing s.r.o., Czech Republic) with online UV-VIS detection by SPECORD® 200 Plus (Analytik Jena GmbH, Germany). About 40 mg of the powder API was dispersed in the 900 mL of 72,4 mM phosphate buffer about pH 6.8 with 0,005 w/V % of TWEEN® 20. The used dissolution method was the paddle

method (USP II) with the rotation speed of paddles being 100 min^{-1} for 45 minutes and then 150 min^{-1} for 15 minutes. API content was detected at 270 nm, and the absorbance was measured after 2, 5, 10, 15, 20, 25, 45 and 60 minutes of the dissolution experiment.

3.3.3. Dissolution of the granules

The dissolution testing was carried out using a dissolution device DS-11 SOTAX (SOTAX Pharmaceutical Testing s.r.o., Czech Republic) with online UV-VIS detection by SPECORD® 200 Plus (Analytik Jena GmbH, Germany). The measured samples were granules (prepared by dry granulation process) containing 40 mg of enzalutamide (amorphous or crystalline). The granules contained 2 % of sodium croscarmellose and a mixture of enzalutamide (crystalline or amorphous) with HPMC AS in ratio 1:2 (F1 – with amorphous enzalutamide, F6 – with crystalline enzalutamide), 1:3 (F2 – with amorphous enzalutamide, F7 – with crystalline enzalutamide), 1:4 (F3 – with amorphous enzalutamide, F8 – with crystalline enzalutamide), 1:5 (F4 – with amorphous enzalutamide, F9 – with crystalline enzalutamide), 1:6 (F5 – with amorphous enzalutamide, F10 – with crystalline enzalutamide). . The dissolution medium was 900 mL of 72,4 mM phosphate buffer with pH about 6.8. The used dissolution method was the paddle method (USP II), with the rotation speed of paddles being 100 min^{-1} for 45 minutes and then 150 min^{-1} for 15 minutes. API was detected at 270 nm, and the absorbance was measured after 2, 5, 10, 15, 20, 25, 30, 35, 40, 45, 50, 55, 60, 65, 70, 75, 80, 85, 90, 95, 100, 105, 110, 115, 120, 125, 130, 135, 140, 145, 150, 155, 160, 170, 180, 190, 200, 210 and 220 minutes.

4. Main results

Two topics are discussed within the dissertation. The first one is related to the preparation and stability of amorphous enzalutamide. The discussed types of preparation of amorphous enzalutamide are DSC, rotary vacuum evaporator, hot melt extrusion, and spray drying. Preparations are discussed with regard to crystallization, which was studied using differential scanning calorimetry. This topic also contains kinetic data of the amorphous enzalutamide, which was exposed to short and long-term stability testing. Other aspects which are discussed are storage conditions (influence of the temperature and humidity), packaging material, optimal preparation process etc.

The second topic is focused on the comparison of the dissolution behavior of the amorphous and crystalline samples. The difference was shown along with the fast crystallization of amorphous drugs. This issue of fast crystallization was solved by adding a water-soluble polymer, which can maintain a supersaturation state.

This thesis covers the crystallization of the amorphous enzalutamide prepared by hot melt extrusion and the study of the dissolution behavior of the material prepared by hot melt extrusion.

4.1. Crystallization of amorphous enzalutamide in solid-state

The amorphous enzalutamide was tested according to the classification of Baird et al. The enzalutamide belongs to class III regarding GFA, which is demonstrated in figure 1. A. The amorphous sample prepared in DSC does not crystallize during the reheating. However, the mechanical stress applied during the grinding generates nuclei, and then the exothermic crystallization occurs on the DSC curve during the reheating (Figure 1B). Kinetic calculations can describe exothermic crystallization. The amorphous enzalutamide presented in Figure 1 is model since DSC preparation is made on a smaller scale than in practice.

Amorphous enzalutamide was prepared by hot melt extrusion, slow solvent evaporation (thermal evaporation on the rotary vacuum evaporator) and spray drying. In case of the hot melt extrusion, two batches were prepared: One batch represents extrudates cooled down to room temperature while exiting the extruder. Second batch was cooled down by liquid nitrogen. The standard kinetic analysis was done for each material. Comparing these different preparation routes showed that solvent evaporation on the rotary vacuum evaporator does not lead to fully amorphous material, and the amorphous structure is looser than material prepared in other ways. The hot melt extrusion and spray drying led to the fully amorphous material, but the most stable one was probably spray-dried sample despite having particle sizes about 0.1 – 1 µm. However, the stability of spray-dried material was not proven by stability testing.

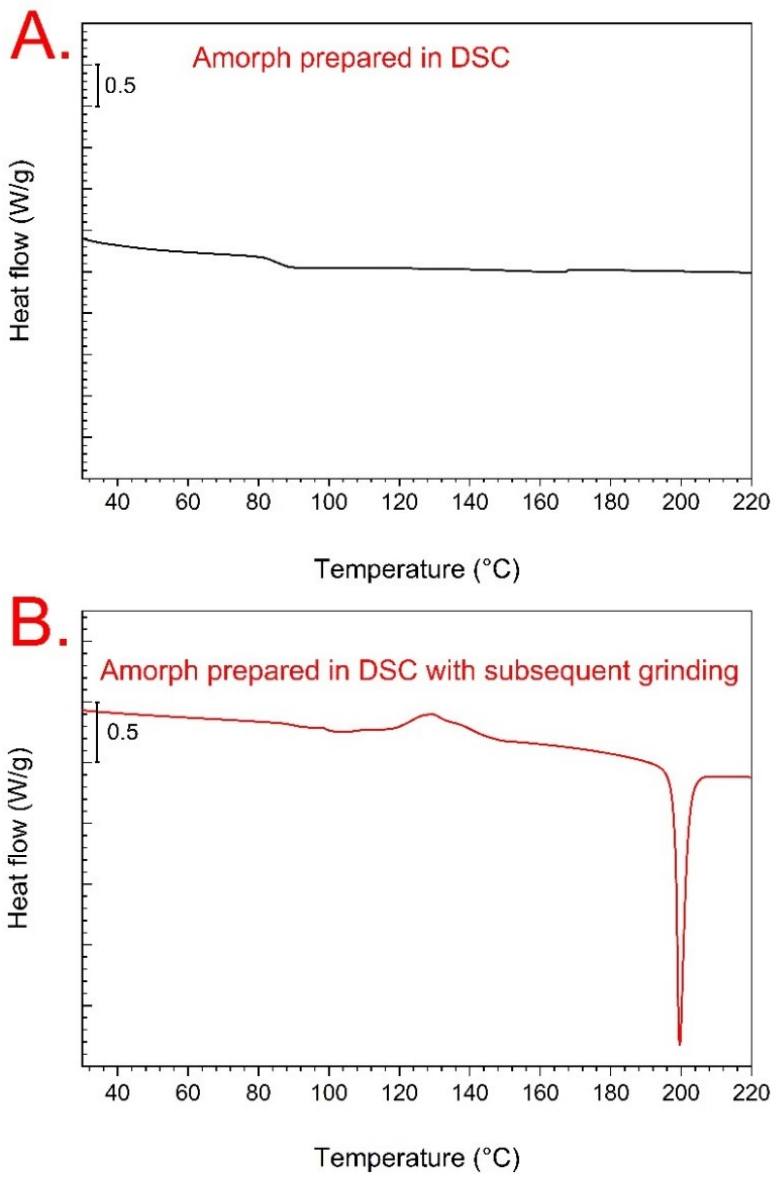

Figure 1. DSC curves taken at 10 °C·min^{-1}: A. amorphous enzalutamide prepared by heating in DSC with subsequent cooling, B. amorphous sample prepared in DSC in the same manner as material displayed in Figure A, but the sample was crushed in agate mortar after cooling.

Comparing hot melt extruded materials, the material that was cooled down to the room

temperature was more stable than the one cooled to the liquid nitrogen temperature, which was proved by the value of activation energy. Other important study included in the dissertation was focused on examining the influence of particles size on the crystallization behavior of the amorphous enzalutamide. The materials compared were spray-dried material with particle sizes about 0.1 – 1 μm and extruded materials divided into a few fractions: 20–50, 50–125, 300–500 μm. DSC curves taken at 10 °C are shown in Figure 2. The figure points out that the crystallization behavior of the spray-dried material is on the same level as the extruded material with markedly bigger particles. In case of the extruded material, crystallization onset shifts to lower temperatures with decreasing particle size. The shift is caused by the mechanical stress, not just by the particle size difference. The smallest fraction (i.e. 20–50 μm) of particles contains the largest amount of mechanical stress. This fact leads to acceleration of crystal growth and occurrence of crystals of different morphology. Despite the spray-dried material having the smallest particles, crystallization behavior is similar to the crystallization of the biggest particles of the extruded material. Mechanical stress plays a major role in the crystallization acceleration. However, crystallization can be predicted based on the parameters of the DSC curve. But, the usual extruded material from the manufacture production contains a wide range of particles size. Then, the prediction can be complicated. However, in this dissertation, the possibility for prediction of the crystallization of raw batch was verified. As was shown in the published articles in the scope of the dissertation, the data taken at 0.5 °C·min^{-1} most resemble the reality.

The Šesták-Berggren model was determined as the most flexible kinetic model for the description of crystallization behavior.

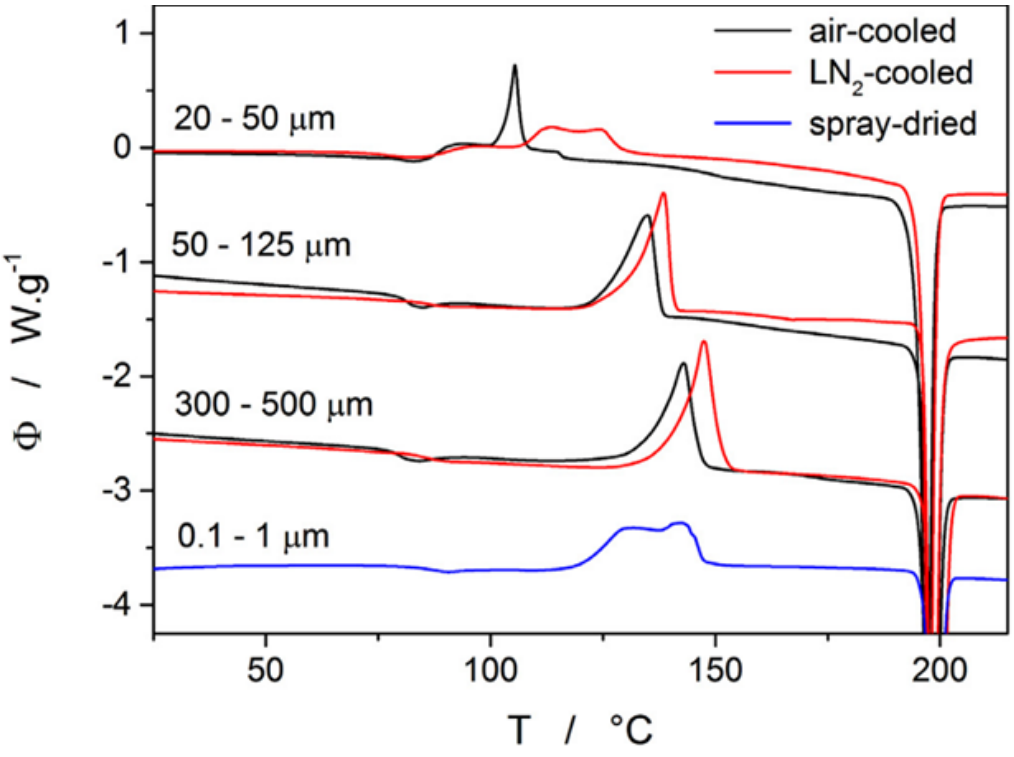

Figure 2. DSC curves of the extruded material cooled to the room temperature (air-cooled, black curves), extruded material cooled by liquid nitrogen (LN2-cooled, red curves) and spray dried material (blue curve). DSC curves were taken at 10 °C min^{-1}. The particle size ranges of the measured materials are shown above each DSC curve.

Table 1 shows the parameters of the DSC curve, which were determined based on the standard kinetic analysis. These parameters were used for isothermal predictions.

Table 1. Kinetic parameters were determined by the modified single-curve MKA applied to the kinetic data obtained at 0.5 °C·min^{-1} (these values were used for the kinetic predictions of isothermal crystal growth).

ID	**air-cooled HME**			**LN_2-cooled HME**			**SD**
d/µm	20–50	50–125	300–500	20–50	50–125	300–500	0.1–1
E /kJ·mol^{-1}	163.1	159.8	162.6	144.7	133.2	139.5	187.0
log(A)/s	22.28	19.06	19.26	19.21	15.87	16.13	24.26
M	0.612	0.538	0.757	0.530	0.791	0.701	0.568
N	0.757	0	0	0.797	0	0	1

The crystallization kinetics depends significantly on the particle size. Therefore, the study included in the dissertation explores the possibility of the combined kinetic predictions weighted by the actual distribution of the particular powder fraction being able to describe the crystallization signal for the as-prepared powdered (unsieved) amorphous Enzalutamide. In the dissertation theses, the two approximations were used for the description of the DSC data of the air-cooled HME material using a combination of the predictions. In the first approximation, the three predictions (20–50 µm, 50–125 µm, 300–500 µm) were used for calculations. The experimental data were fit (using non-linear optimization) by the predictions with the weighing factors being variable (see Figure 3B):

$$\alpha_{exp} = \sum w_i \cdot \alpha_{pi} \tag{11}$$

$$\sum w_i = 1 \tag{12}$$

where α_{exp} represents the experimentally obtained data, α_{pi} are the individual theoretical predictions for the given d_{aver}, and w_i are the corresponding weighting factors. The result of the best fit is represented by the red dashed line in Fig. 3F.
In the second approximation, added predictions for the following particle size fractions typically prepared in our lab: 125–180, 180–250 and 250–300 µm. The predictions were derived/calculated via arbitrary interpolation of the kinetic parameters obtained for the two boundary fractions (50–125 and 300–500 µm):

$$P_i = \frac{k_i}{4}(P_{300-500} - P_{50-125}) + P_{50-125} \tag{13}$$

where Pi is the value of the kinetic parameter (E, A, M or N) for ith powder size fraction, P300–500 and P50–125 are the values of that parameter for the indexed fractions, and ki is 1, 2 and 3 for the 125–180, 180–250 and 250–300 µm fractions. In this way, a series of gradually slowed down crystallization processes was implemented into the non-linear optimization in the 50–500 µm d_{aver} range. The corresponding fit of the experimental
data is shown by the blue line in Fig. 3B. To conclude, reasonable predictions can be made based on the knowledge of the kinetic parameters-see full version of the

dissertation thesis. The predictions were also correlated with the results of the stability testing, and the predictions are very accurate. In addition, the prediction can be calculated for any raw material while the particle distribution is experimentally found out.

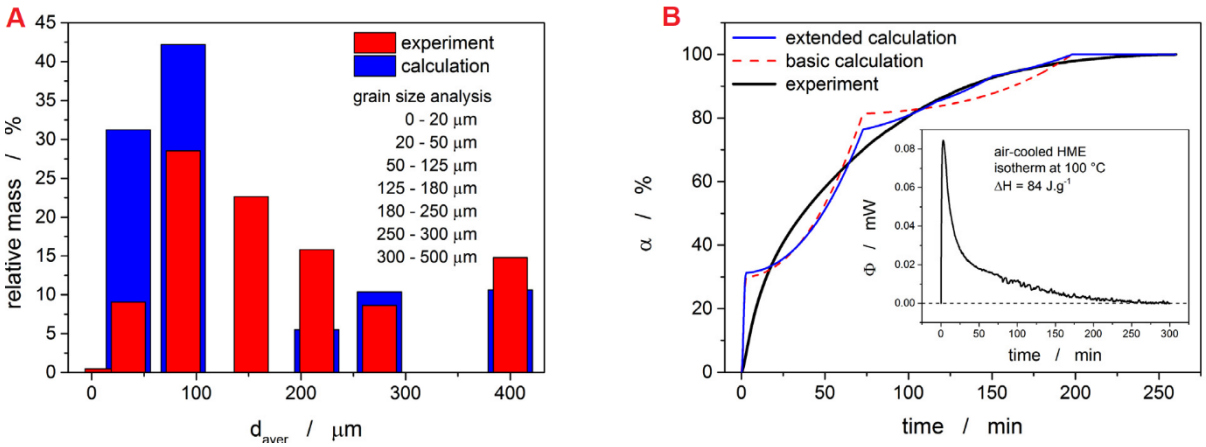

Figure 3. E) Results of the particle size analysis for the air-cooled HME-produced Enzalutamide (red columns). Theoretical particle size distribution (blue columns) calculated on the basis of the extended non-linear optimization fitting the isothermal annealing data of the unsieved material with the extended kinetic predictions of the d_{aver} fractions investigated in this work (blue line in graph F), F) Black line - isothermal crystallization α-t dependence of unsieved air-cooled HME-produced Enzalutamide (details of the experiment and raw DSC data are shown in the inset). Red dashed line – fit of the experiment via the three base kinetic predictions corresponding to the kinetic results of the 20–50, 50–125 µm and 300–500 µm particle size fractions. Blue line – fit of the experiment via the kinetic predictions corresponding to the three experimentally obtained kinetic datasets (for the 20–50, 50–125 and 300–500 µm powder fractions) and three other datasets, theoretically calculated for 125–180, 180–250 and 250–300 µm powders.

The following paragraphs summarize some findings of the dissertation related to the crystallization of enzalutamide. All studies focused on the crystallization of enzalutamide aimed to develop a standard procedure for the investigation of crystallization of amorphous APIs. If the amorphous enzalutamide is prepared in DSC in small scale, the exothermic crystallization is not observed on the DSC curve during the heating of the amorphous form. If the amorphous enzalutamide is prepared by hot-melt extrusion then the grinding of the extrudates generates nuclei, then the exothermic crystallization is observed on DSC curve. The crystallization of extruded material is not dependent on the particle size. However, it depends on the level of mechanical stress. If the amorphous enzalutamide is prepared by spray drying, then the generation of nuclei is probably caused by the residual solvent. The spray-dried amorphous enzalutamide seems to be more stable than extruded one. The dissertation results proved the reliability of the mathematical prediction of crystallization even below the temperature of glass transition. The additivity of the crystallization signals for the powder material with different particle sizes was also verified. It was proved that the extruded material crystallizes independently on temperature and humidity. The amorphous extruded material crystallizes even et 5 °C. Therefore, the only important factor is mechanical stress. On the contrary, the spray-dried material stays amorphous for six months at 5 °C.

4.2. Dissolution of enzalutamide

Apparent intrinsic dissolution (USP VI) revealed that amorphous extruded material (air-cooled HME) has six times higher intrinsic dissolution rate than crystalline form (polymorphic form R1). The dissolution behavior of amorphous form in powder form was examined using the paddle method (USP II). In the powder form, advantage of the amorphous form was neglected due to immediate precipitation with subsequent crystallization. The dissolution curves (paddle speed 50 rpm) are shown in the full dissertation theses. The dissolution behavior of the crystalline form corresponds to first-order kinetics according to the equation:

$$A_t = 2.51\left(1 - exp(-0.08t)\right) \quad (14)$$

where A_t corresponds to the dissolved amount, t is time.

On the contrary, dissolution behavior of the amorphous form corresponds to zero-order kinetics:

$$A_t = 0{,}07t + 0{,}46 \quad (15)$$

where A_t corresponds to the dissolved amount, t is time.

To maintain higher apparent solubility of the amorphous form, hydroxypropyl methylcellulose acetate succinate was added into the formulation. In order to achieve immediate release, the granules were prepared with 2 wt. % of disintegrant. The granules were prepared with different ratio of API and polymer. The dissolution profiles of granules containing amorphous or crystalline enzalutamide with hydroxypropylmethylcellulose are shown in Figure 4. Obviously, the HPMC AS inhibits precipitation/crystallization of amorphous enzalutamide and enable gradual dissolving of enzalutamide. The data were fitted to two kinetic models. The first one was the first-order kinetic model, the high determination coefficients (R^2 = 0.9564 – 0.9895) were achieved in the case of formulation with amorphous enzalutamide. The lower determination coefficients (R^2 = 0.7811 – 0.9524) in comparison to formulation with amorphous enzalutamide were observed in case of formulation with crystalline enzalutamide. In case of enzalutamide generally, the determination coefficient decreases with the increasing amount of polymer. However, the increasing amount of polymer (HPMC AS) in formulation increases the value of the dissolution rate constant in both cases (amorphous enzalutamide, crystalline enzalutamide). About 7.5 – 10 times higher amount of enzalutamide was dissolved from the formulation with amorphous enzalutamide compared to formulation with crystalline enzalutamide within the dissolution section of 60 minutes. The value mentioned in the previous sentence was determined as the quotient of the maximum releasable amount during 60 minutes from the granules with the amorphous form to the maximum releasable amount from the granules with crystalline form. The amount of HPMC AS in the formulation have a negligible influence on the value of the maximum releasable amount. The difference between the maximum releasable amount in the boundary ratios (F1 compared to F5, F6 compared to F10) of formulation with amorphous enzalutamide (F1 compared to F5) was 3,9 wt. % and the difference in the case of formulation with crystalline enzalutamide was 1.5 wt. %. However, the highest amount of dissolved enzalutamide was observed in the case of formulation F3, F5 and F5, where the ratio between the amorphous enzalutamide and HPMC AS was 1:4, 1:5 and 1:6.

The second kinetic model used for the fit of the dissolution curves was model Korsmeyer-Peppas. The observed values of release exponents were lower than 0.5, which indicates a diffusion-driven dissolution mechanism.

The granules consisting of amorphous enzalutamide, HPMC AS, and sodium croscarmellose (disintegrant) can be eventually filled into gelatin capsules and used as potential formulation.

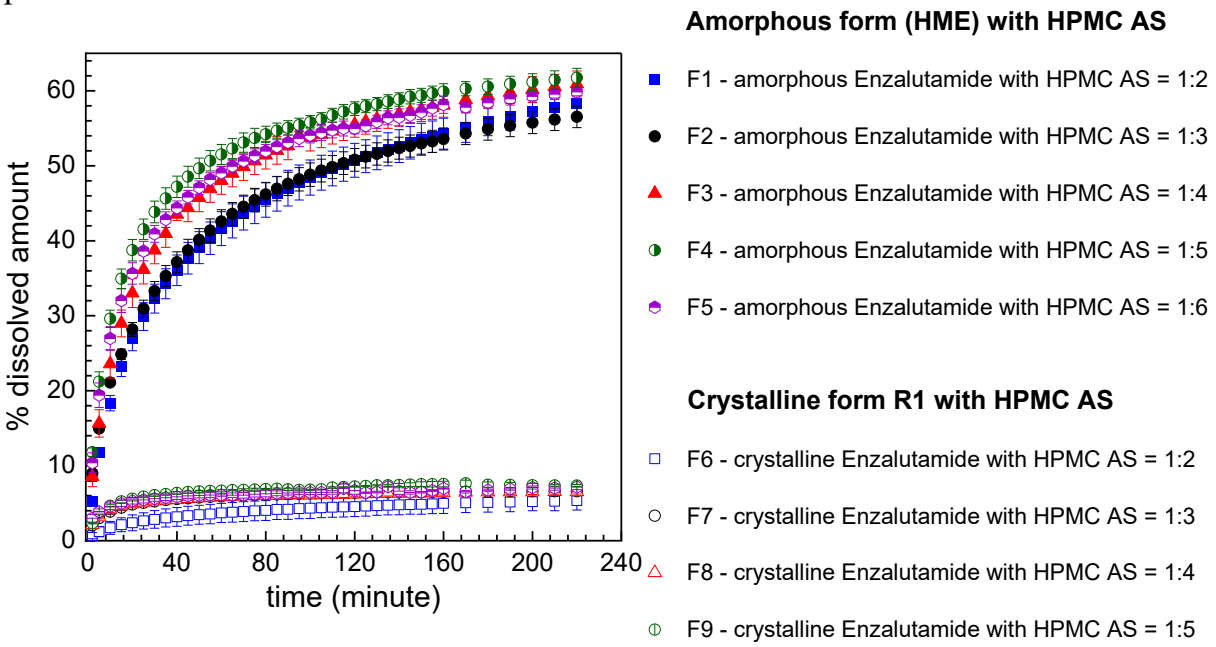

Figure 4. Dissolution of the granules containing amorphous (HME) or crystalline enzalutamide (polymorphic form R1) and HPMC AS in ratios 1:2, 1:3, 1:4, 1:5 and 1:6. The formulation contains in addition 2 wt. % of sodium croscarmellose.

5. Conclusion

The dissertation is focused on the description of the solid-state stability of amorphous enzalutamide and its dissolution behavior. The amorphous enzalutamide was classified as API belonging to class III, according to GFA (***G****lass* ***F****orming* ***A****bility*). The mechanical activation of the API surface (grinding, milling, etc.) plays a major role in the acceleration of the enzalutamide's crystallization. The comparison of the amorphous enzalutamide prepared by different routes showed that the presence of the mechanically induced nuclei is critical for crystallization. One of the aims of the dissertation theses was the characterization of the crystallization kinetics of the amorphous API and prediction of the crystal growth. The isothermic experiments are time-consuming; therefore, the modelling based on the non-isothermal experiments was verified. The theoretical predictions were confirmed by experimental results, what is shown in the full version of the dissertation. The most reliable predictions were gained based on the parameters determined using the lowest heating rate during non-isothermal experiments.

The second part of the dissertation was focused on the examination of the difference between the dissolution of amorphous and crystalline enzalutamide. The basic difference is in the dissolution rate of pure forms. The amorphous form dissolves six times faster than the crystalline form. However, the dissolution of samples in powder form shows also fast precipitation with immediate crystallization. This event

negated the benefit of amorphous form. The benefit can be kept by preparation of the granules with HPMC AS and other excipients. The HPMC AS can maintain the enzalutamide dissolved and also can inhibit the crystallization of the amorphous form of enzalutamide. The HPMC AS enables the dissolution of 7.5 – 10 times larger amount of enzalutamide from the amorphous form than the crystalline form. The dissolution rate constant increases with the higher amount of HPMC AS, so immediate release can be achieved. The granules with HPMC AS can be used as filling of the gelatin capsules.

The dissertation shows the model study of amorphous API belonging to class III according to GFA. The main purpose of the dissertation was determination of technological and physicochemical parameters of this API. The preparation, processing, and long-term storage conditions were simulated and experimentally tested in the first part of the work. The second part of the work was focused on the procedure needed for testing the dissolution behavior of this API when the suppression of the precipitation with crystallization was a major aim. Both topics showed the significant instability of drugs belonging to class III according to GFA and possible solutions to this issue.

6. List of References

(1) Blaabjerg, L. I.; Lindenberg, E.; Rades, T.; Grohganz, H.; Löbmann, K. Influence of Preparation Pathway on the Glass Forming Ability. *International Journal of Pharmaceutics* **2017**, *521* (1–2), 232–238. https://doi.org/10.1016/j.ijpharm.2017.02.042.

(2) Rams-Baron, M.; Jachowicz, R.; Boldyreva, E.; Zhou, D.; Jamroz, W.; Paluch, M. *Amorphous Drugs*; Springer International Publishing: Cham, 2018. https://doi.org/10.1007/978-3-319-72002-9.

(3) Charalabidis, A.; Sfouni, M.; Bergström, C.; Macheras, Panos. The Biopharmaceutics Classification System (BCS) and the Biopharmaceutics Drug Disposition Classification System (BDDCS): Beyond Guidelines. *International Journal of Pharmaceutics* **2019**, *566*, 264–281. https://doi.org/10.1016/j.ijpharm.2019.05.041.

(4) Willart, J. F.; Descamps, M. Solid State Amorphization of Pharmaceuticals. *Mol. Pharmaceutics* **2008**, *5* (6), 905–920. https://doi.org/10.1021/mp800092t.

(5) Baird, J. A.; Van Eerdenbrugh, B.; Taylor, L. S. A Classification System to Assess the Crystallization Tendency of Organic Molecules from Undercooled Melts. *Journal of Pharmaceutical Sciences* **2010**, *99* (9), 3787–3806. https://doi.org/10.1002/jps.22197.

(6) Alhalaweh, A.; Alzghoul, A.; Kaialy, W.; Mahlin, D.; Bergström, C. A. S. Computational Predictions of Glass-Forming Ability and Crystallization Tendency of Drug Molecules. *Mol. Pharmaceutics* **2014**, *11* (9), 3123–3132. https://doi.org/10.1021/mp500303a.

(7) Mahlin, D.; Bergström, C. A. S. Early Drug Development Predictions of Glass-Forming Ability and Physical Stability of Drugs. *European Journal of Pharmaceutical Sciences* **2013**, *49* (2), 323–332. https://doi.org/10.1016/j.ejps.2013.03.016.

(8) Cabral, A. A.; Fredericci, C.; Zanotto, E. D. A Test of the Hrubÿ Parameter to Estimate Glass-Forming Ability. *Journal of Non-Crystalline Solids* **1997**, *219*, 182–186. https://doi.org/10.1016/S0022-3093(97)00327-X.

(9) Van Eerdenbrugh, B.; Baird, J. A.; Taylor, L. S. Crystallization Tendency of Active Pharmaceutical Ingredients Following Rapid Solvent Evaporation—Classification and Comparison with Crystallization Tendency from Under Cooled Melts. *Journal of Pharmaceutical Sciences* **2010**, *99* (9), 3826–3838. https://doi.org/10.1002/jps.22214.

(10) Descamps, M.; Willart, J. F.; Dudognon, E.; Caron, V. Transformation of Pharmaceutical Compounds upon Milling and Comilling: The Role of T(g). *J Pharm Sci* **2007**, *96* (5), 1398–1407. https://doi.org/10.1002/jps.20939.

(11) Babu, N. J.; Nangia, A. Solubility Advantage of Amorphous Drugs and Pharmaceutical Cocrystals. *Crystal Growth & Design* **2011**, *11* (7), 2662–2679. https://doi.org/10.1021/cg200492w.

(12) *Principles and Applications of Thermal Analysis*; Gabbott, P., Ed.; Blackwell Publishing: UK, 2008.

(13) Liu, X.; Lu, M.; Guo, Z.; Huang, L.; Feng, X.; Wu, C. Improving the Chemical Stability of Amorphous Solid Dispersion with Cocrystal Technique by Hot Melt Extrusion. *Pharm Res* **2012**, *29* (3), 806–817. https://doi.org/10.1007/s11095-011-0605-4.

(14) Wellen, R. M. R.; Canedo, E. L. On the Kissinger Equation and the Estimate of Activation Energies for Non-Isothermal Cold Crystallization of PET. *Polymer Testing* **2014**, *40*, 33–38. https://doi.org/10.1016/j.polymertesting.2014.08.008.
(15) Starink, M. J. The Determination of Activation Energy from Linear Heating Rate Experiments: A Comparison of the Accuracy of Isoconversion Methods. *Thermochimica Acta* **2003**, *404* (1–2), 163–176. https://doi.org/10.1016/S0040-6031(03)00144-8.
(16) Šesták, J.; Berggren, G. Study of the Kinetics of the Mechanism of Solid-State Reactions at Increasing Temperatures. *Thermochimica Acta* **1971**, *3* (1), 1–12. https://doi.org/10.1016/0040-6031(71)85051-7.
(17) Arhangel`skii, I. V.; Dunaev, A. V.; Makarenko, I. V.; Tikhonov, N. A.; Tarasov, A. V. Non-Isothermal Kinetic Methods. **2013**.
(18) Avrami, M. Kinetics of Phase Change. I General Theory. *The Journal of Chemical Physics* **1939**, *7* (12), 1103–1112. https://doi.org/10.1063/1.1750380.
(19) U.S. Food and Drug Administration https://www.fda.gov/home (accessed 2021 -10 -17).
(20) European Medicines Agency https://www.ema.europa.eu/en (accessed 2021 -10 -17).
(21) *Český Lékopis*; Grada Publishing: Praha, 2017.
(22) Yu, L. X.; Amidon, G. L.; Polli, J. E.; Zhao, H.; Mehta, M. U.; Conner, D. P.; Shah, V. P.; Lesko, L. J.; Chen, M.; Lee, V. H. L.; Hussain, A. S. Biopharmaceutics Classification System: The Scientific Basis for Biowaiver Extensions. *Pharmaceutical Research* **2002**, *19* (7), 921–925. https://doi.org/10.1023/A:1016473601633.
(23) Hezaveh, H.; Muhamad, I. I. Controlled Drug Release via Minimisation of Burst Release in PH-Response Kappa-Carrageenan/Polyvinyl Alcohol Hydrogels. *Chemical Engineering Research and Design* **2013**, *91* (3), 508–519. https://doi.org/10.1016/j.cherd.2012.08.014.
(24) Costa, P.; Sousa Lobo, J. M. Modeling and Comparison of Dissolution Profiles. *European Journal of Pharmaceutical Sciences* **2001**, *13* (2), 123–133. https://doi.org/10.1016/S0928-0987(01)00095-1.
(25) Huang, X.; Brazel, C. S. On the Importance and Mechanisms of Burst Release in Matrix-Controlled Drug Delivery Systems. *Journal of Controlled Release* **2001**, *73* (2–3), 121–136. https://doi.org/10.1016/S0168-3659(01)00248-6.
(26) Al-Zoubi, N.; Malamataris, S. Three-Layer Matrix Tablets and Simple Approach of Drug Release Programming. *Journal of Drug Delivery Science and Technology* **2008**, *18* (6), 431–437. https://doi.org/10.1016/S1773-2247(08)50083-9.
(27) Peppas, N. A. Analysis of Fickian and Non-Fickian Drug Release from Polymers. *Pharm Acta Helv* **1985**, *60* (4), 110–111.
(28) Wyttenbach, N.; Kuentz, M. Glass-Forming Ability of Compounds in Marketed Amorphous Drug Products. *European Journal of Pharmaceutics and Biopharmaceutics* **2017**, *112*, 204–208. https://doi.org/10.1016/j.ejpb.2016.11.031.

7. List of published papers

Published papers related to the dissertation:

Paper I
Romanová, J.; Svoboda, R.; Obadalová, I.; Beneš, L.; Pekárek, T.; Krejčík, L.; Komersová, A. Amorphous Enzalutamide – Non-Isothermal Recrystallization Kinetics and Thermal Stability. *Thermochimica Acta* 2018, *665*, 134–141. https://doi.org/10.1016/j.tca.2018.05.020.

Paper II
Svoboda, R.; **Romanová, J.**; Šlang, S.; Obadalová, I.; Komersová, A. Influence of Particle Size and Manufacturing Conditions on the Recrystallisation of Amorphous Enzalutamide. *European Journal of Pharmaceutical Sciences* 2020, *153*, 105468. https://doi.org/10.1016/j.ejps.2020.105468.

Other published papers:

Paper III
Brandová, D.; Svoboda, R.; Zmrhalová, Z. O.; Chovanec, J.; Bulánek, R.; **Romanová, J.** Crystallization Kinetics of Glassy Materials: The Ultimate Kinetic Complexity? *J Therm Anal Calorim* 2018, *134* (1), 825–834. https://doi.org/10.1007/s10973-018-7078-1.

Paper IV
Knapik-Kowalczuk, J.; Kramarczyk, D.; Chmiel, K.; **Romanova, J.**; Kawakami, K.; Paluch, M. Importance of Mesoporous Silica Particle Size in the Stabilization of Amorphous Pharmaceuticals—The Case of Simvastatin. *Pharmaceutics* 2020, *12* (4), 384. https://doi.org/10.3390/pharmaceutics12040384.